Chapter 3. Second-harmonic generation of Nd:YAG laser

1. Introduction

1.1. General review

Frequency up-conversion is very important in nonlinear optics. Optical second-harmonic generation(SHG) was the first nonlinear effect discovered with the help of lasers.

Franken and coworker[1] used ruby laser to pump crystalline quartz and observed the second-harmonic wave in their pioneer. The next important step in the study of second-harmonic generation was the work of Giordmaine[2] and Maker[3] who undertook experimental investigation of the free and forced waves and proposed an effective method of phase matching in optics.

Since then, numerous works about the generation of second-harmonic waves were done on about three aspects: The first is the development of the theory of wave interactions in dispersive nonlinear media. These works were based on optical harmonic generators itself with the purpose of making it more high efficient. For the harmonic generation by plane monochromatic waves, it was shown that the spatial and temproral modulation of waves decreases the efficiency of harmonic genrators. It goes without saying that one of the most important results in this aspect was the discovery of the principles of optimum focusing. The theory of this kind of optimum focusing(generally in Gussian profile) was nearly completely constructed so far.

The second is the searching for new materials which were

used for these nonlinear optical experiments. Although the quartz used in the pioneering work of Franken and co-workers was proved to be unsuitable for constructing ferquency multipliers(because of non-fulfilment of phase-matching conditions). Efficient materials for nonlinear interaction in the visible and near ultraviolet ranges were found as far back as 1962, in particular, KDP and ADP crystals used firstly by Giodmaine and Maker in their experiments.[2,3] Many other nonlinear crystals have been found in the course of the past 60's and 70's, starting with $LiNbO_3$, BNN, LI and HIO_3. Interesting results were obtained by Patel[4] who constructed an experiment on SHG with a CO_2 laser. He found that the nonlinear susceptibility of Te is approximately 10^3 times larger than that for KDP, which now formed the base for far infrared sources.

In the last decade, some new nonlinear materials with its transparency range in the spectrum of ultraviolet and visible and infrared were discovered. New nonlinear optical materials in borate system, typically LBO and BBO were discovered in 1985[5]. The works searching for new materials are now in the ascendent.

For efficient frequency conversion one must ensure that the phase velocities of the interacting waves are all the same so that the signal may build up in intensity at the expense of the pump radiation throughout the whole of the medium. Thus the researching works on phase matching theories and methods were the third main aspect synchronical

as the first and the second. Giordmaine and Maker independently showed that one method of phase matching at the fundamental and the harmonic waves for a SHG experiment in KDP was to utilize the birefringence and the dispersive properties of the crystal[2,3]. Midwinter and Warner[6] systematically discribed the effects of phase matching method and of uniaxial crystal symmetry on the polar distribution of second-order nonlinear optical polarization. Some other new methods for phase-matching were discovered, as we have discribed in chapter 1, such as phase-matching in homogeneous isotropic media with anomalous dispersive, phase-matching due to rotary double refraction and in periodic and inhomogeneous systems. Quasi-phase-matching aforementioned in chapter 2 is one of the typical examples.

1.2. SHG in LN crystal with PDS

Periodic reversal of the sign of nonlinear coefficient of the material at coherence length prevents the accumulation of phase mismatch between the interacting waves. In LN crystal, as we have discussed in chapter 1, nonlinear coefficient is modulated spatially with the PDS in which its period corresponds to coherence length. Different fundamental wavelength corresponds to different coherence length. Thus for frequency doubling of a given fundamental source, the corresponding period of domain structures in LN is required. We show the calculated relationship between the fundamental wavelength and coherence length in LN crystal in

which the fundamental light propagates along the a-axis in fig.1. In near IR, the most common fundamental source is the Nd:YAG laser and the diode laser, thus the fabrication of such frequency doubler for those sources are of practical significance. In the earily 1980s, Feng and co-workers[7]

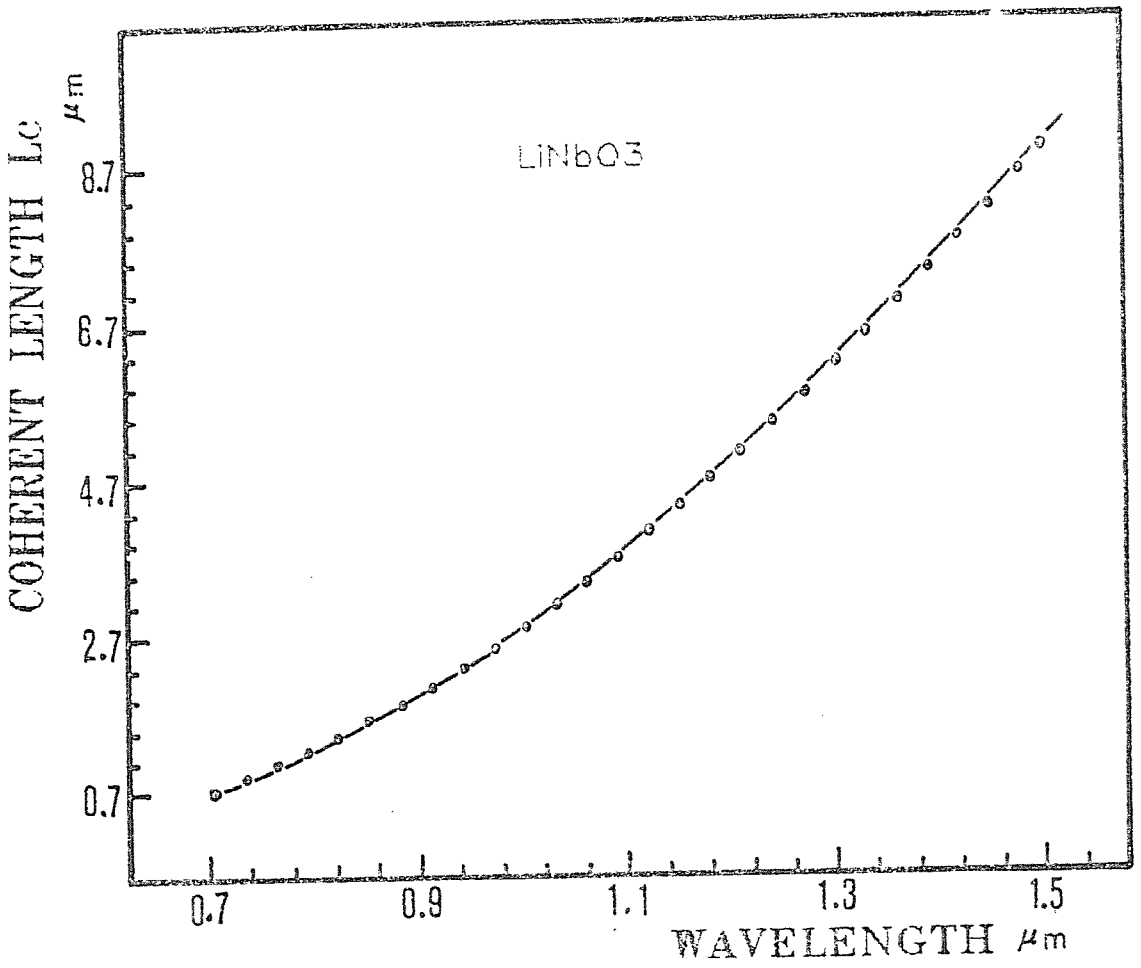

Fig. 1. The relationship between the fundamental wavelength and coherence length in LN crystal (fundamental light propagates along a-axis).

succeeded in achieving enhanced SHG efficiency of Nd:YAG laser based on QPM in $LiNbO_3$ crystal with periodic laminar ferroelectric domains. They have grown this kind of material with about 200 laminas in 1984[8]. Using d_{33} nonlinear

coefficient, they have tested an enhancement factor of about 16.9 times larger than that of using d_{31}, and the square relationship between the number of domain laminas and second-harmonic wave intensity, i.e. equation (1.1), was verified. Feist also reported the similar works for Cr-doped LN crystal in which the number of domain laminas they used was about 50 in 1985.[9] SHG in waveguide and crystal fiber which have periodic domain structures have been realized by Byer and Magel[10]. They reported a structures of 230 domain laminas was used to generate blue light by direct doubling of GaAlAs laser diode. This is one of possible methods in fabricating a miniaturized, compact, all-solid blue light sources and will have potential applications in the area ofmost advanced science. We shall present the part of our works in next chapter, In this chapter, we only discribe the SHG of the laser of 1064 nm.

2. Experimental results and discussion

2.1. Experimental setup

Fundamental wave light was generated by a picosecond automatical tunable parametric oscillator with its fundamental power about 0.17 Mw. Fundamental wave light was directly focused into crystal sample using a 40 mm focusing lens. The diameter of light spot at focal plane is about 1 mm. For efficiency measurement of green light (harmonic wave), an infrared light cutting filter was used for blocking the passed infrared light behind the crystal

sample. The experimental setup is shown in figure 2. The oscillator uses KDP crystal as working material and pumped by Nd:YAG laser with three steps magnifications. Because our laser is tunable, so no angle tuning and temperature stabilization equipments are required. In all experiments

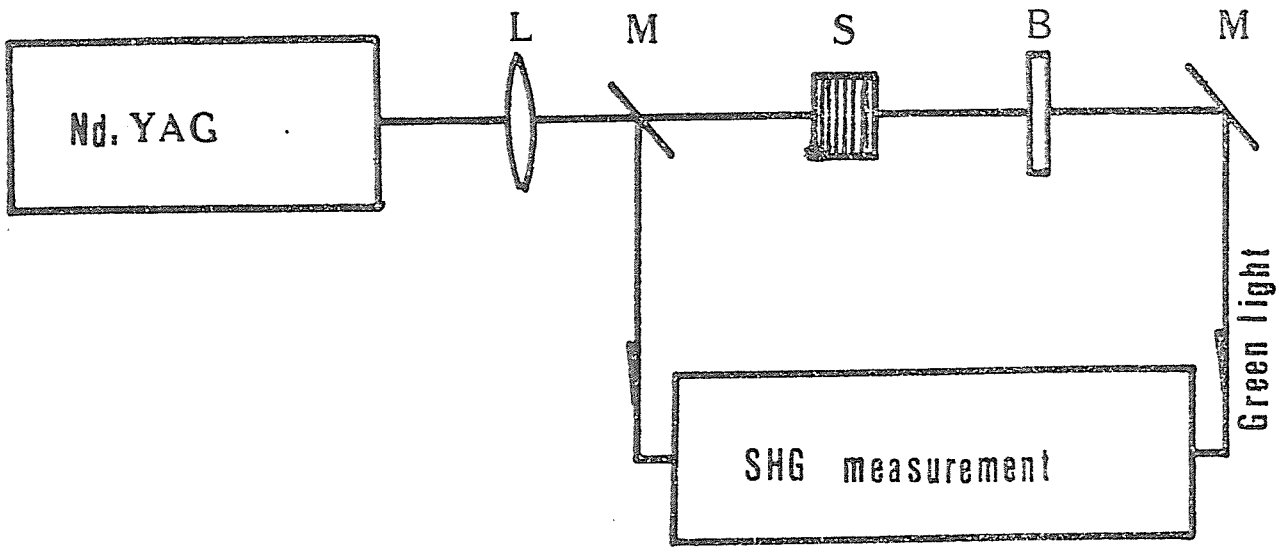

Fig. 2. Experimental setup.

we did, the d_{33} nonlinear coefficient was used for SHG in e+e-->e nonlinear interacting process.

2.2. The quadratic relationship between the number of domain laminas and SHG efficiency

As we have mentioned in the discussion of equation(1.1), one of the most important conclusions in QPM theory is that the quadratic relationship between the number of domain laminas and the SHG efficiency exists. In the earily of

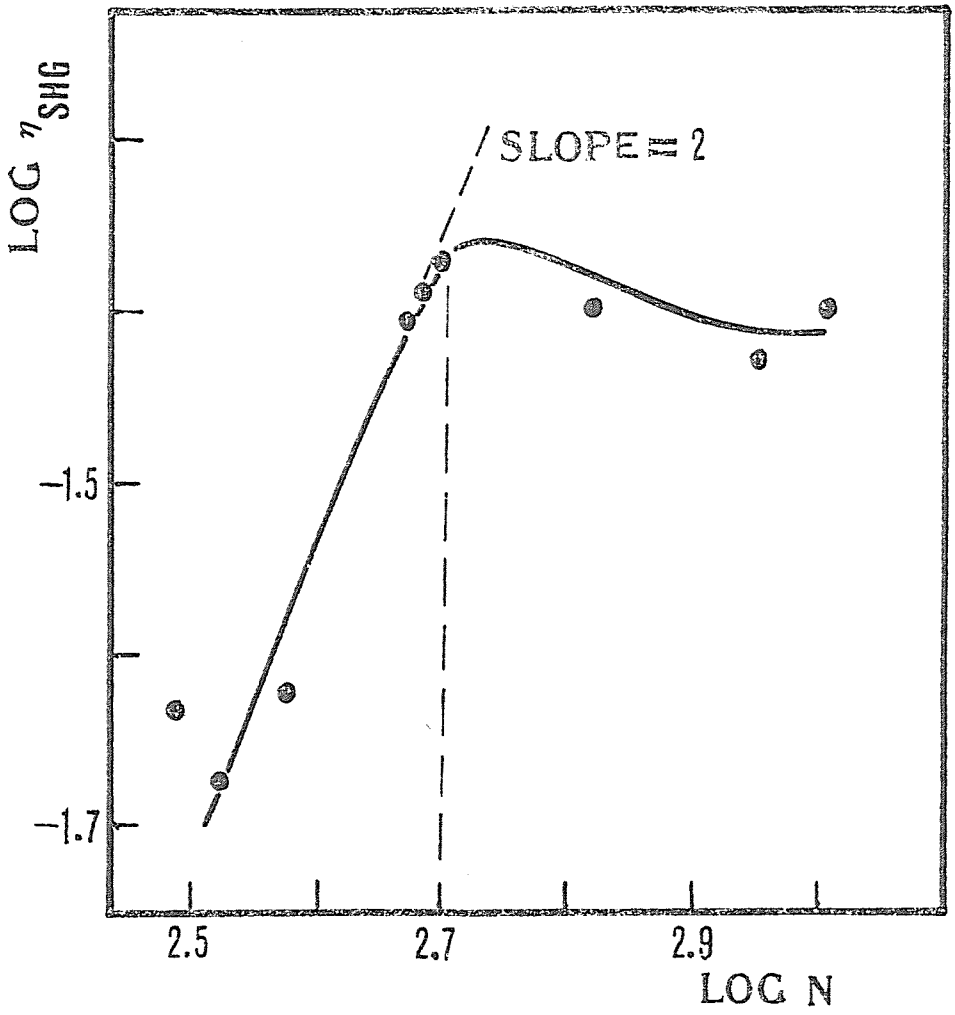

Fig. 3. The quadratic relationship between the number of domain laminas and SHG efficiency.

1982, Xue et.al has verified the relation up to about 200 laminas.[8] Feisst has done the same experiment in the scope of 50 laminas.[9] In their experiments, the results were in

good agreement with the above theory. But with large number of domain structures, they shown the great discrepancy between the results of experiments and the theory. This was intepreted as the inhomogeneity and the discontinueity of laminar domain structures. Thus the verification of the relationship can reflect the advance in growing the LN crystal with PDS. All our experimental works are shown in fig.3. All the points shown in this figure are normalized at the same pumping power and the same pumping wavelength. Up to 500 domain lamina, the quadratic relationship is approximately satisfied. When the number of domain laminas beyond 500, great discrepancy exists, as the previous work shown. Many factors, such as the existance of island-like domains, the discontinuity of the PDS, the inequality between the positive and the negative domain laminas and the experimental errors, etc., can be the origins of the discrepancy. These factors introduce a correction on the number of domain laminas, N, then the effective number of domain laminas reduced. It will give a reduction on SHG efficiency. With our sample of good regularity of the period distribution which it has about 600 domain laminas, over 11% conversion efficiency of Nd:YAG laser was obtained in our experiment with the input energy of 5 μj. The conversion efficiency is comparable to that in 0.9 mm long commercial single domain LN crystal.

2.3. Effective number of domain laminas and SHG efficiency--- characterization of the PDS in LN crystal

As the equation (1.2), the amplitude of second-harmonic wave of electric field is as follows:

$$E_{2\omega} = \frac{8\pi d_{33}}{n_{2\omega}^2 - n_{\omega}^2} T R^2 E_{\omega}^2 \cdot \left| \sin\left(\frac{\pi l'}{2 l_c}\right) \cdot \sum_{m=1}^{N} (-1)^{m-1} \cdot \exp\{-i(m-1)\pi l'/l_c\} \right| \quad \ldots(3.1)$$

in which we define the effective number of domain laminas:

$$N_{eff} = \left| \sin\left(\frac{\pi l'}{2 l_c}\right) \sum_{m=1}^{N} (-1)^{m-1} \exp\{-i(m-1)\frac{\pi l'}{l_c}\} \right| \quad \ldots(3.2)$$

For $l' = l_c$, then $N_{eff} = N$, which is for the ideal case. For the case of $l' \neq l_c$, then the $N_{eff} < N$, which is for the practical case. Here l' is the thickness of each domain laminar and the summation is over all periodic domain structures. then the equation (1.1) can be writen as:

$$I(2\omega)/I_0(2\omega) = N_{eff}^2 \quad \ldots(3.3)$$

For a contineous structures, two factors on the material itself which determine the l' in above equation(or N_{eff}) are:

a). The inequality between the thickness of the positive and the negative laminar domains. For a given fundamental wavelength, l' is not equal to l_c, but the relation of $l_p + l_n = 2l_c$ is satisfied in the case when QPM condition holds.

b). The unstability of the period of the domain structure. In this case, the $l_p + l_n$, for a given fundamental wavelength, can not be equal to $2l_c$, and thus the QPM condition is not

satisfied.

In practical case, all the two factors can exist in the samples. By carefully choicing the growing parameters, the first factor above, as we have discribed in chapter 2, can be avoided, and thus can be neglected in considering the effective number of domain laminas. Only the second factor, i.e., the distribution of the period of domain structures should be considered.

N_{eff} is also a function of fundamental wavelength. For a given period distribution of domain structures, different fundamental wavelength corresponds to different N_{eff}. The relation is:

$$N_{eff} = \left| \sum_{m=1}^{N} (-1)^{m-1} \exp\left\{ \frac{-2i(m-1)\pi l'(n_{2\omega} - n_{\omega})}{\lambda} \right\} \right| \qquad \ldots(3.4)$$

From this equation, for a given period distribution, we can calculate the realtionship between N_{eff} and the fundamental wavelength . The relationship gives the information about fundamental wavelength at which the QPM condition is best satified and which it corresponds to the largest N_{eff}. Thus it gives a method for characterization of the PDS. To verify our analysis given above, two experiments can be proposed: the first is the SHG efficiency measurements on fundamental wavelength scanning. This experimental results in a form of scanning curve is comparable, according to equation (3.3), with the calculated relationship between the N_{eff} and the fundamental

wavelength.

The second method is the SHG efficiency measurements with fundamental wavelength scanning at different rotating angle of sample which the angle is that between the normal of sample surfaces and the propagation direction of fundamental wavelength. For a given sample, different angles means different period distribution(for a rotation angle of Q, the period becomes 1/cosQ of the original period). Then the scanning measurements of SHG efficiency at different angles will give us much details about the PDS in LN crystal.

In the following two sections, we will discuss the SHG efficiency measurements with fundamental wavelength scanning and these measurements at different rotating angles . The calculated relationship between N_{eff} and the fundamental wavelength for each case mensioned above are given in each corresponding section.

2.3.2. The relationship between the fundamental wavelength and N_{eff} or SHG efficiency

The SHG efficiency measurements with fundamental wavelength scanning were made on Sample A. Sample A has thickness of 1.56 mm and the observed number of domain laminas is 480. The thickness of the positive domain laminas is nearly equal,to that of the negative. The period distribution of the sample which was measured by optical microscope, was shown in fig.4. For simplicity of

calculation, we have shown this contineous change of period distribution as steps changes. For each step, there is an average thickness l' of domain laminas and its number of domain laminas N'. Thus from equation (3.4), the N_{eff} for different fundamental wavelength can be oatained.

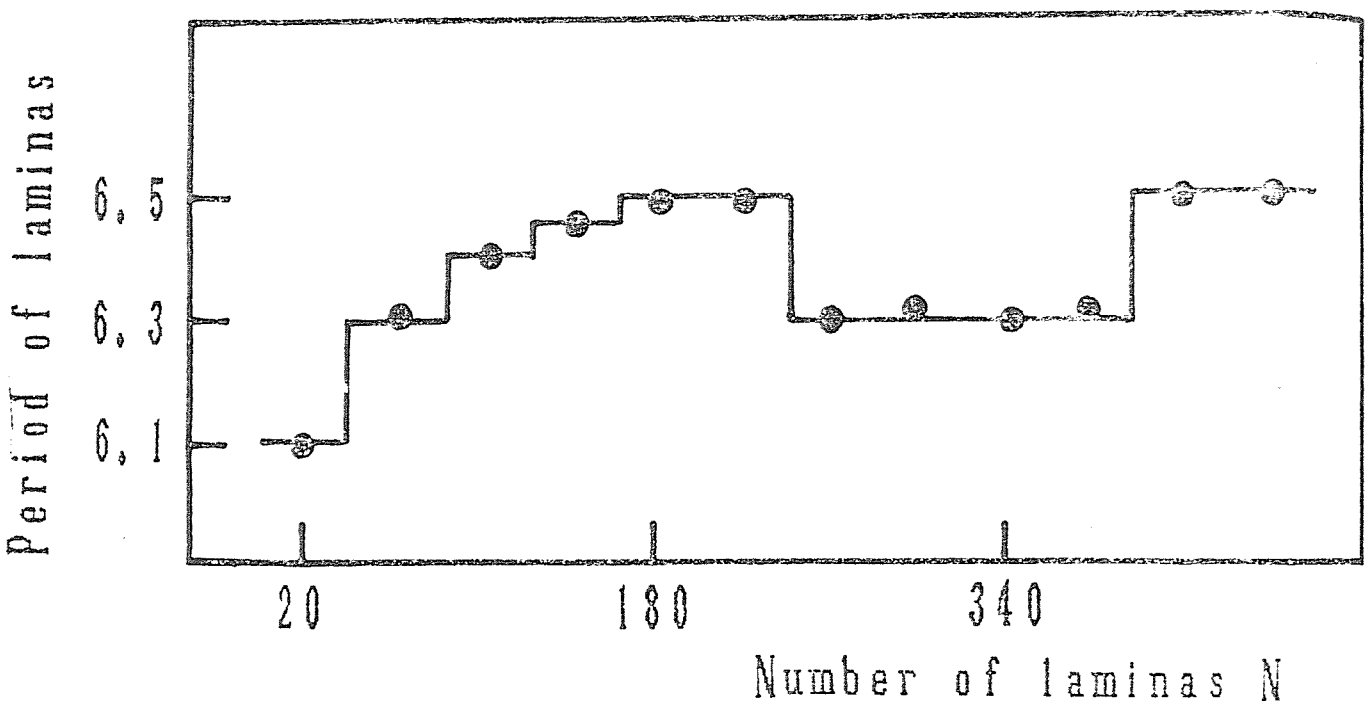

Fig. 4. The period distribution of domain structures in sample A.

Fig.5 shows the experimental curve of SHG efficiency vs the fundamental wavelength. Three peaks are easily seen in this curve, this shows that the regularity of period distribution of the domain structures is very poor in sample A.

The calculated relationship of N_{eff}^2 as the fundamental wavelength have been shown in fig.6, the three peaks are also evidently existed in this curve. We have listed the

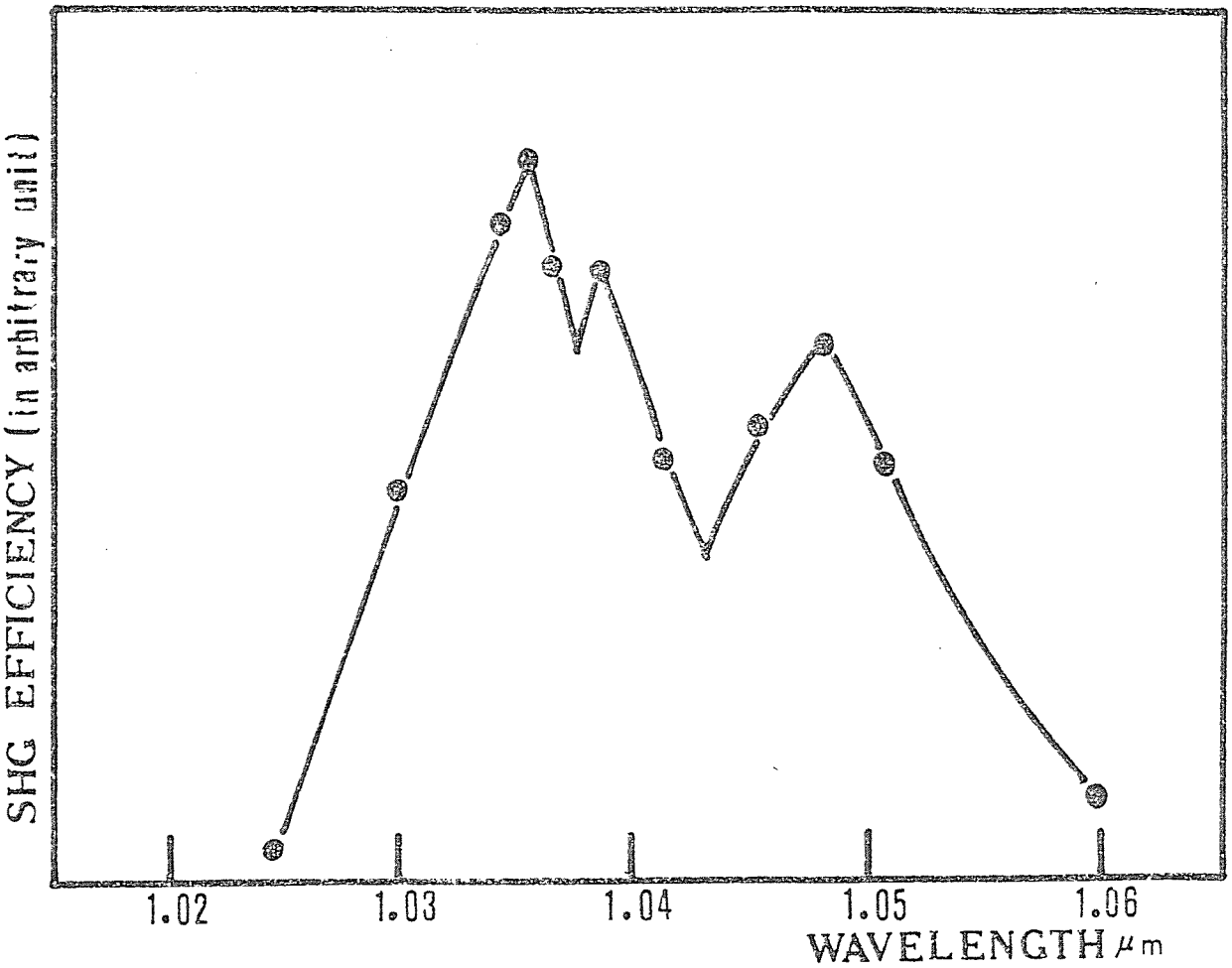

Fig. 5. The experimental curve of SHG efficiency vs fundamental wavelength.

wavelengthes at which the three peaks occured for the case of measured and calculated in table 1. The results corresponds very good.

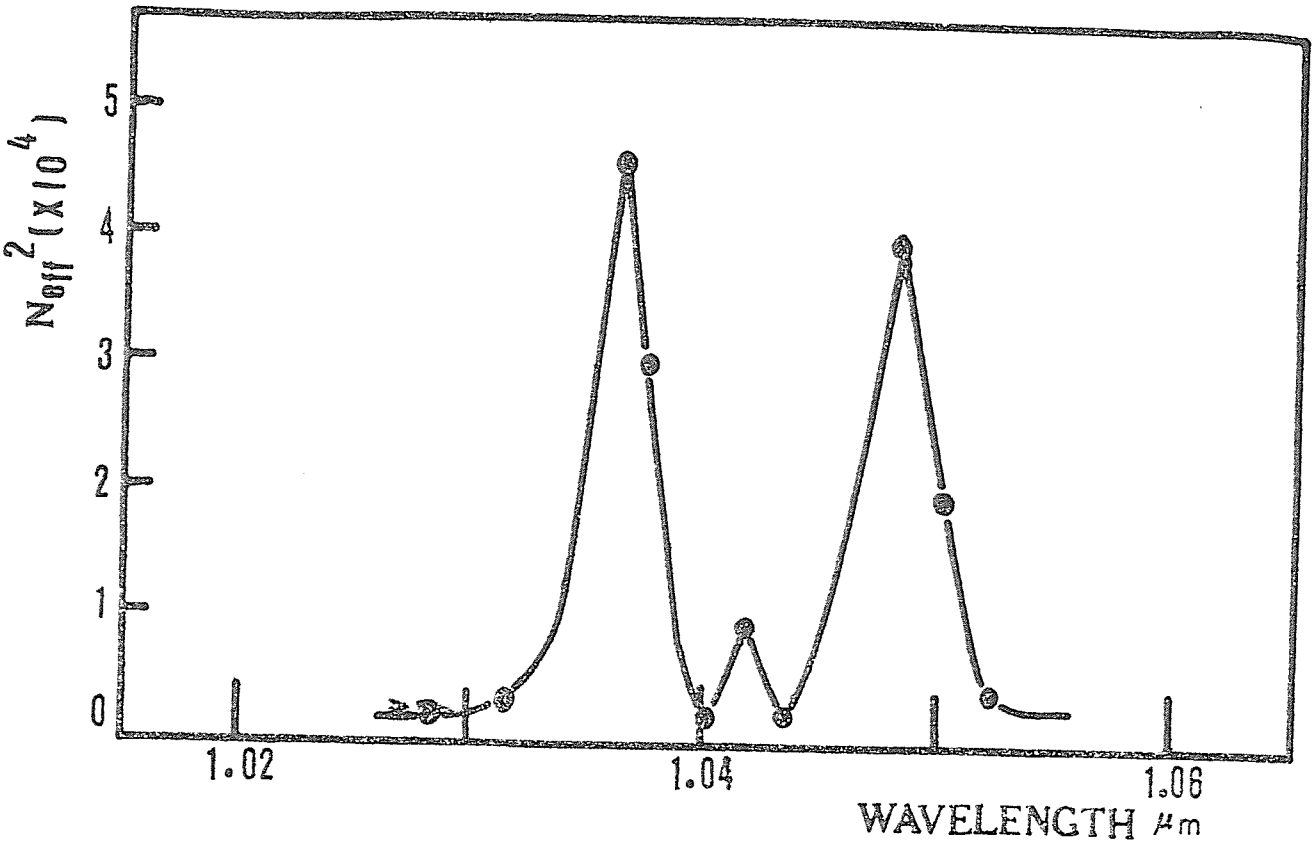

Fig. 6. The calculated curve of N_{eff}^2 vs fundamental wavelength .

Table. 1. The correspondence of results in scanning curves of the measured and the calculated.

Measured wavelength(μm)	1.035	1.040	1.048
Calculated wavelength (μm)	1.036	1.042	1.048
N_{eff} (at peaks)	218	91	211
Correspoding l_c(μm)	3.15	3.21	3.27

In this table, the maximal effective number of domain laminas N_{eff} is 218, it is very smaller than the actual

number of the domain laminas of 480. This shows that the regularity of period distribution is very important for characterizing the LN crystal with PDS.

In conclusion of this section, we should point out that, even though the N is 480 in sample A, the N_{eff} can be nearly equal to zero for certain fundamental wavelength, as shown in fig.6. This indicates the importance of achieving phase matching in SHG process.

2.3.3. The relationship between the fundamental wavelength and N_{eff} or SHG efficiency at different rotation angles

We took sample B for the SHG efficiency measurements with the fundamental wavelength scanning at different rotation angles. Sample B has thickness of 2.15 mm and the observed number of domain laminas is 660. The thickness of the positive domain laminas is also nearly equal to that of the negative. we shown in fig.7 the period distribution which is also expressed as step changes.

The experimental results are shown in fig.8. Four curves correspond to four rotation angles of 0°, 5°, 10°, and 15° respectively, as we have marked in this figure. In fig.8, the curve for 0° angle has the highest SHG efficiency. SHG efficiency decreases as the rotating angle increases. When the angle exceeds about 10°, the SHG efficiency decreases abruptly. The curve becomes more diffusive as the rotating angle increases.

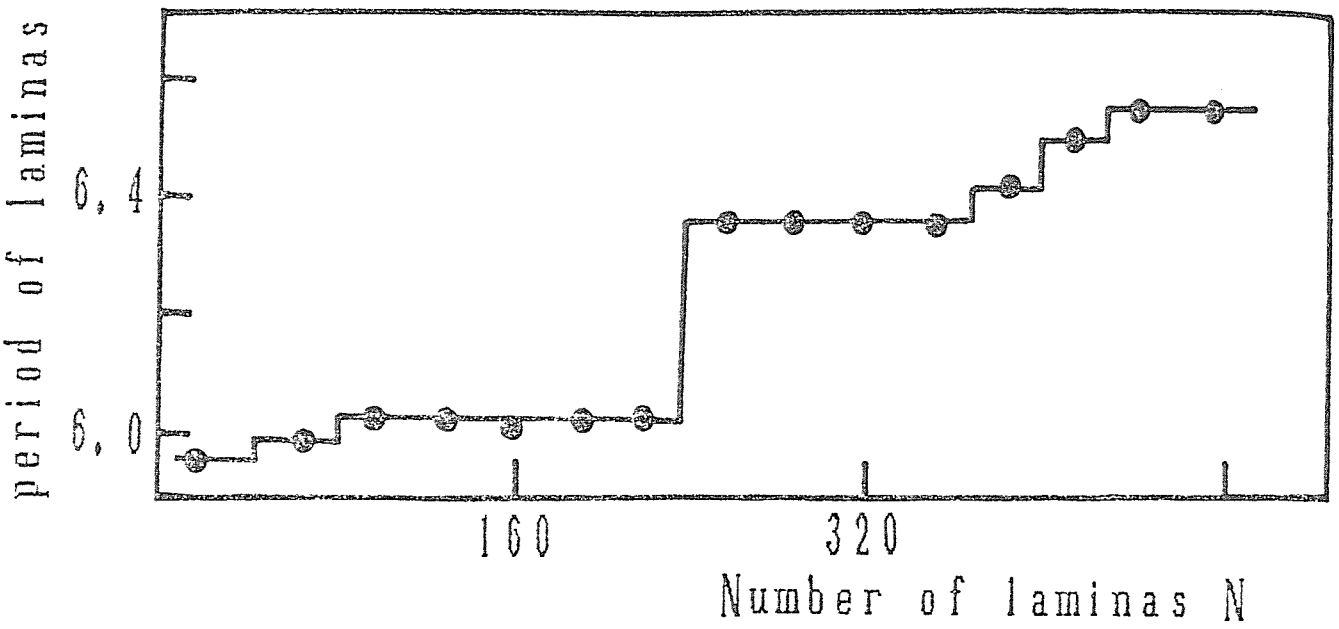

Fig. 7. The period distribution of domain structures in sample B.

The calculated relationship between SHG efficiency and fundamental wavelength at different rotating angles are shown in fig.9. It should point out that we have only shown here the part of calculation curves in which the fundamental wavelength is in the range of 1020 nm to 1035 nm, though the measurement scope, as was shown in fig.8, was made from 1020 nm to 1060 nm. the broad range of fundamental wavelemgth in sample B is caused by its very diffusive period distribution.

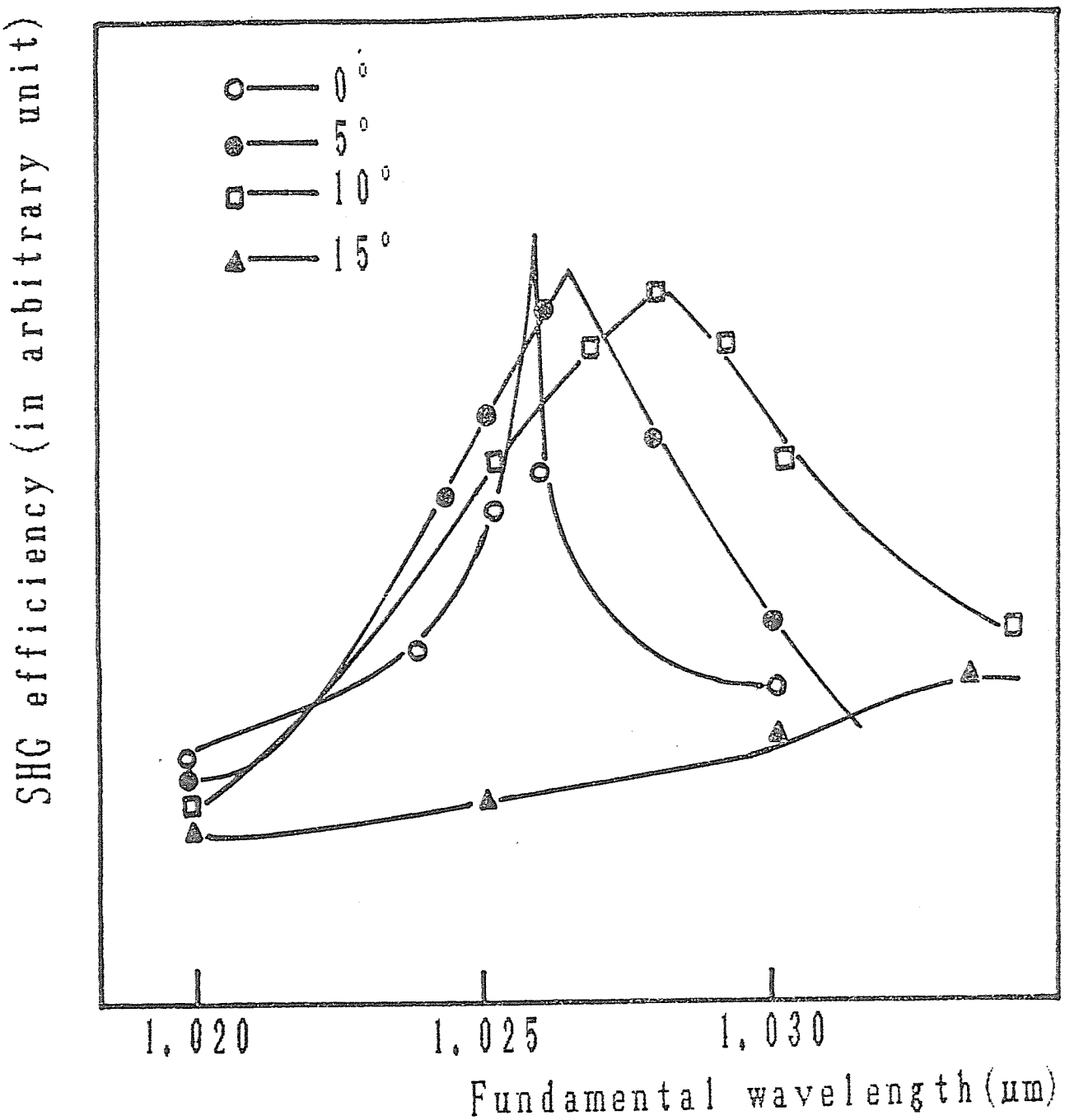

Fig. 8. The experimental curve of SHG efficiency vs fundamental wavelength at different angles.

From fig.8 and fig.9, the maxima are existed in both the experimental and the calculated curves at different rotating angles. we list in table 2 the results of wavelengthes at where the maxima appears and the effective numbers of domain laminas.

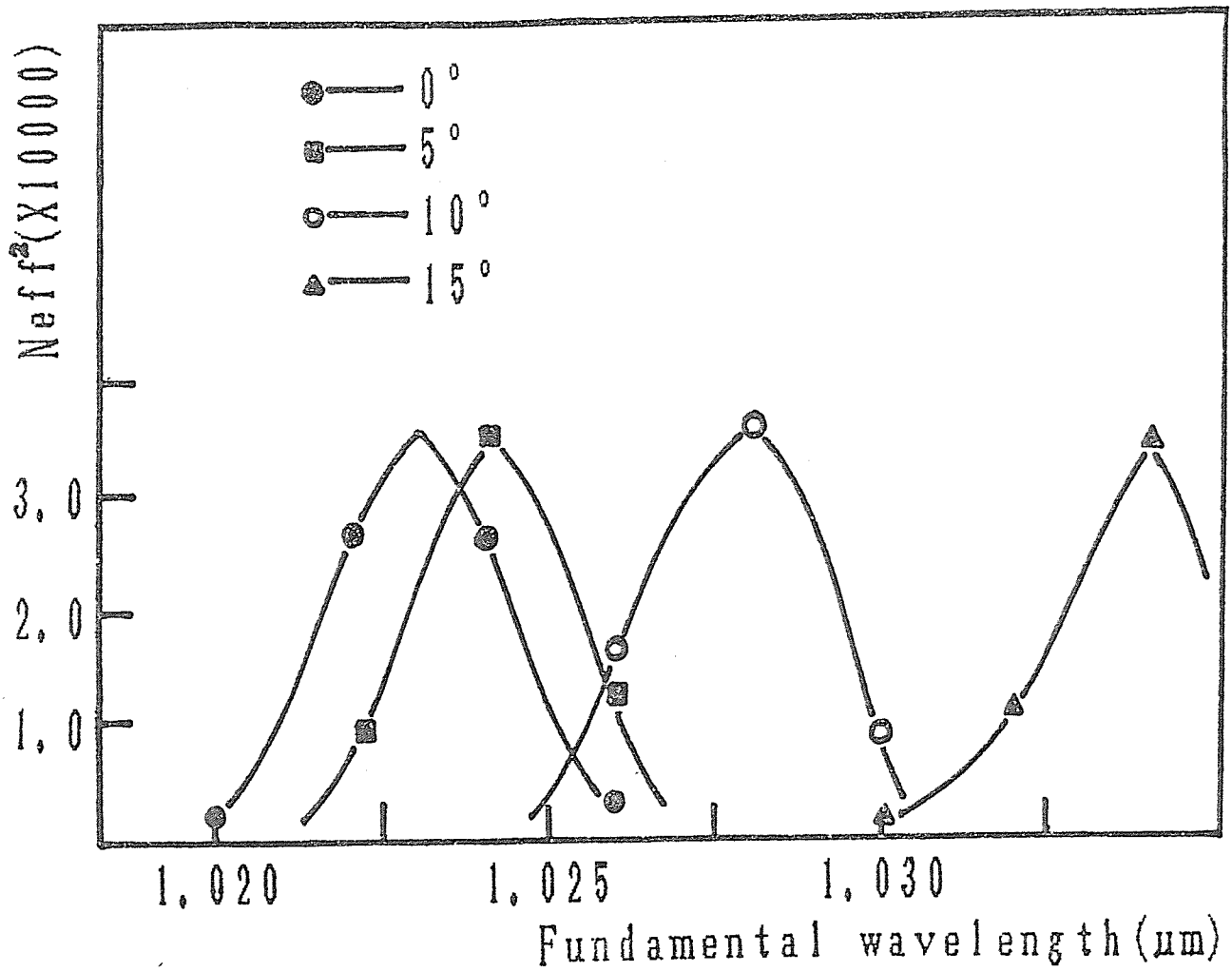

Fig. 9. The calculated curve of N_{eff}^2 vs fundamental wavelength at different angles.

Table 2. The results for SHG efficiency measurements and calculations in scanning experiments

Angle of rotation(deg.)	0	5	10	15
Measured wavelength (for maximal) (μm)	1.025	1.026	1.028	1.033
Calculated wavelength (μm)	1.023	1.024	1.028	1.034
N_{eff}	165	187	188	188
Corresponding l_c	3.01	3.04	3.07	3.13

Comparing the maximal effective number of domain laminas of 188 in this table, with the practical N of 660, it shows that the sample B has a more bad regularity of the period distribtuion than that of sample A. The two samples with bad regularity of the period distribution were choiced for verifying our calculations.

2.3.4. Discussion

As what were shown in equation (3.3), N_{eff} can effectively reflect the SHG efficency variation with the fundamental wavelength. We have discussed the results in last two sections. But the lineshape of both the measured and the calculated scanning curves is different in our results given above. This is caused by our step approximation of the period distribution of domain structures. If more steps are used for calculation, more accurate results can be obtained. However, the calculation relationship between N_{eff} and the fundamental wavelength by step approximation can effectively offer the information such as the fundamental wavelength for

best QPM condition, corresponding N_{eff}, etc. It gives us an important conclusion of whether the sample has the value of practical applications.

If we take the absorption or the reflection of the fundamental wave light in sample in our calculation, a very important result, which is the tolerance angle beyond which the SHG efficiency decreases abruptly, can be obtained. But in the above calculations there is no result in this aspect in fig.9 because we have not considered the absorption or reflection effects. In fig.8, we have experimentally obtained the tolerance angle which is about 10°. With antireflection coating layer on the sample, the tolerance angle could be greatly increased. We will use the tolerance angle of 30° in calculating of the tuning curves of optical parametric oscillation in chapter 5.

The tolerance angle is important for its practical applications of LN crystal with PDS in which the sample rotation is required for achieving exact QPM condition.

3. Concluding remarks

In this chapter we demostrated the possibility of practical application of the LN crystal with PDS in SHG with high conversion efficiency. We have measured the SHG efficiency variation while the number of domains changes. The quadratic relationship was verified quantitatively to 500 laminas.

The fundamental wavelength scanning in SHG efficiency measurement can reflect the periodicity of the sample. From the distribution of the domain structures, we can calculate the relation between the effective number of domains and the fundamental wavelength variation. The results show that the calculation is very effective for evaluating the periodicity of the sample and deciding at what wavelength the QPM occures. The recording of the scanning curves by rotating the sample at different angles can offer the information about the tolerance angle tolerance for the practical applications of the crystals.

Reference:

1. P.Franken. A.Hill. C.Petars. Phys.Rev.Lett. 7 (1961)118

2. J.A. Giordmaine. Phys.Rev.Lett. 8 (1962)19

3. P.D.Maker. R.W Terhune. Phys. Rev.Lett. 8 (1962)21

4. C.K.N. Patel. Phys. Rev.Lett. 15 (1965)1027

5. C.T. Chen et.al. Sci.Sin.Ser. B28(1985)235

6. J. E. Midwinter and J.Warner Brit. J.Appl.Phys. 16(1965)1135

7. D.Feng et.at. Appl.Phys.Lett. 37(1980)607

8. Y.H.Xue. et.at. Acta.Phys.Sin. 32(1983)1515

9. A.Feisst and P.Koidl Appl.Phys.Lett. 47(1985)1125

10. G. A. Magel. M.M.Fejer and R.L.Byer. Appl.Phys.Lett. 56(1990)108

Chapter 4. The generation of blue light by SHG

1. Introduction

1.1. Methods for compact blue sources.

1.2. Advances for blue light generation.

1.3. Direct doubling of diode laser by Cherenkov radiation scheme and by QPM

2. Measurements on the generation of blue light

2.1. Sample preparation and the experimental setup

2.2. Measurements of blue light as fundamental wavelength scanning

3. Concluding remarks

1. Introduction

Compact blue laser devices are of interest for a wide variaty of applications, including optical data storage, laser printing, lithography, color displays, and under water communications. Blue semiconductor injection lasers would be very attractive for these applications, but severe fabrication difficulties associated with wide-band gap semiconductor materials have hampered their development. On the other hand, near-infrared GaAlAl diode lasers have become a mature technology and devices with cw output powers in excess of 1 W have been developed. These high power GaAlAs diode lasers are attractive sources for frequency upconversion to visible wavelengths.

1.1. Methods for compact solid-state visible sources

For the generation of blue, blue green, and green light, many methods have been studied in the past, which include:

1).Intracavity SHG of diode-pumped 946nm Nd:YAG laser, which was used to generate blue light 473 nm.

2).Intracavity frequency mixing of 809 nm diode laser and 1064 nm radiation from a diode laser-pumped Nd:YAG laser, which lead to generation of blue light 459 nm.

3).SHG of Nd:YAG laser for the generation of green light 532 nm in $KNbO_3$, KTP, $MgO:LiNbO_3$.

4).Self-frequency doubling in $Nd:MgO:LiNbO_3$ and NYAB crystals for 532 nm green light generation.

5).SHG in the form of Cherenkov radiation in a proton-exchanged $LiNbO_3$ waveguide, which was used to generate blue light.

6).QPM in periodic domain structure $LiNbO_3$ crystal for the generation blue to green light.

7).The direct emmision of semiconductor diode laser, but so far the emmision spectral region of it is in red near 600 nm.

For comparison of these methods, two categories are classified technically in them: the first is the diode laser pumping and the second is the direct doubling of diode laser.

In comparison with the direct output of a diode laser, diode pumped lasers has some advantages. The relatively poor spatial and spectral modes of high-power diode lasers are converted to the TEM_{oo} spatial mode, and the narrow spectrum characteristics of the solid-state laser which permits highly efficient nonlinear interactions. In addition, the nonlinear crystal can be placed inside the solid-state laser cavity to increase the up-conversion efficiency by taking advantage of the high intensity of the intracavity laser field.

But for the generation of blue light, the usage of $KNbO_3$ and KTP crystals for up-conversion of diode pumped lasers have some disadvantages. For low average power nonlinear interaction, KTP has relatively low nonlinearity in comparison with KN crystal. It is difficulty for using KTP

to realized the output power levels necessary for many practical applications. The twins, cracking and other difficulties during crystal growth hampered the availability of KN crystal for nonlinear optical interactions. Also, for achieving phase matching condition, precise control of temperature and angle of the crystal is necessary. This gives additional inconvenience for constructing the miniaturized blue laser. whereas, as a comparison, direct doubling of diode lasers using QPM technique have high efficiency and relatively simple and economic construction of blue lasers. The using of the largest d_{33} nonlinear coefficient of LN make it possible that the realization of output power levels necessary for practical applications.

1.2. Advances for blue light generation

For highly efficient generation of blue light in these nonlinear crystals, phase matching must be achieved. Three methods of phase matching are noncritical phase matching (NPM) in $KNbO_3$,KTP and MgO:$LiNbO_3$, QPM in $LiNbO_3$, $LiTaO_3$ and KTP in the form of bulk and waveguide, and balance phase matching (BPM) in KTP waveguide. Some recent advances in this aspect have been listed in table 1 and table 2. For review articles, see references[1,2].

Table 1. blue lasers from diode/dye-laser pumped systems

laser	pump source	conversion tech.	nonlinear cryst.	output
Nd:YAG	diode-laser	SHG(1)	$KNbO_3$	473 nm
-----	-----	SFM(1)	-----	436 --
-----	-----	SFM(2)	-----	459 --
-----	-----	SFM(3)	-----	455 --
-----	-----	SFM(2)	KTP	459 --
-----	dye-laser	SFM(2)	---	459 --
diode-laser	-----	waveguide	$LiNbO_3$	420 --
-----	-----	DSHG	$KNbO_3$	431,421
-----	-----	----	-----	425-435
OPO	-----	QPM	PPLN	420-532

Notions used in Table 1

SHG(1): intracavity SHG

SFM(1): sum-frequency-mixing of diode(at 809 nm) and diode-pumped Nd:YAG (at 946 nm)

SFM(2): sum-frequency-mixing of diode (at 809nm) and diode-pumped Nd:YAG(at 1064 nm)

SFM(3): sum-frequency-mixing of diode (at 795 nm) and diode-pumped Nd:YAG (at 1064 nm)

DSHG: direct SHG

PPLN: periodically-poled littium niobate

Table 2.

crystal	output (nm)	output power(mw)	input power(mw)	laser	conversion tech.	ref.
KN	432	0.4	14	diode	DSHG	3

Nd:YAB	532	15	350	---	self-doubling	3
KN	428	41	400	---	SHG(1)	4
--	421	24		---	DSHG	5
--	459	1	diode-pumping		SFM(2)	6
KTP	---	1		---	---	7
KN	455	154	270mw at 795 nm 4.5w at 1064 nm	---	SFM(3)	8
waveguide $LiNbO_3$	420	1.05	120	diode	Waveguide	9

1.3. Direct doubling of diode laser by Cherenkov radiation scheme and QPM

In order to increase the conversion efficiency for the generation of blue light, large nonlinearity of crystal is required. As aforementioned, the d_{33} coefficient of $LiNbO_3$ is very large and then the use of d_{33} of LN is of importance for high efficient SHG. There are two schemes which are under developing at present. The first is guided wave optical devices through Cherenkov radiation, and the second is QPM in both bulk and waveguide materials, both in $LiNbO_3$ crystal using the d_{33} coefficient.

1). Waveguide devices

The d_{33} nonlinear coefficient can be used in the form of Cherenkov radiation, where the phase matching occurs between the guided mode and radiation mode[10]. Precise temperature control is unnecessary for harmonic generation. Also, when the waveguide is proton-exchanged, the optical damage

threshold increases, allowing for higher input power, thus increases the efficiency.[11]

The blue light source is configurated as shown in figure 1 of a diode laser, focusing elements, a half wave plate, and a proton-exchanged $LiNbO_3$ waveguide as the frequency doubler. This half-wave plate is necessary to convert the TE

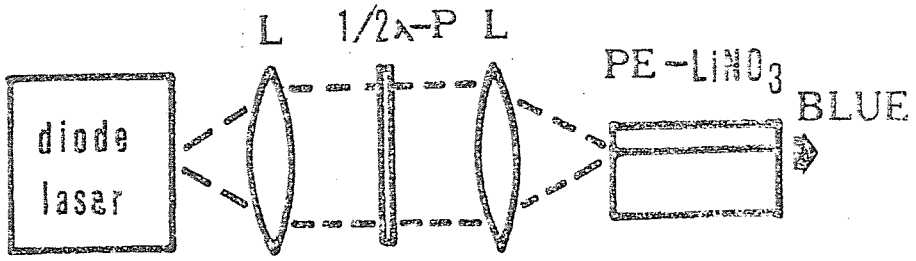

Fig. 1. The construction of blue laser using proton-exchanged LN waveguide.

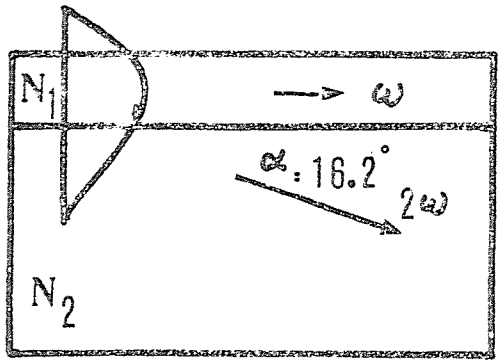

Fig. 2. Cherenkov scheme in waveguide.

mode from the diode laser to the TM mode for propagation in the waveguide. Cherenkov radiation, as shown in figure 2, is caused by the fact that the nonlinear polarization in the waveguide has a phase velocity exceeding that of the radiation propagating in the substrate. therefore the phase matching is achieved between the guided mode and the radiation mode.

2). Quasi-phase-matching

The basic concept of QPM method have been discussed in previous chapters. We only review here its application in the generation of blue light. Research on this subject is just at the beginning. Magel[12] of Stanford university has grown small-diameter single crystal of $LiNbO_3$ with periodic domain structures by laser-heated pedestal growth. The diameter of crystal is about 250 μm. With about 230 laminas, they measured a maximum conversion efficiency of 8×10^{-5}. This efficiency was obtained with 3 mW of input fundamental power and 6.7 μW of blue light generated in this crystal.

Lim[13] et.al have obtained 1 μW of blue light output at 425nm generated from diode laser of 189 mW by QPM method.

In this chapter, we shall discuss the picosecond blue light generation in our researches.

2. Measurements of the generation of blue light

2.1. Sample preparation and the experimental setup

The z-cut as-grown crystals were first etched with 1HF:2HNO_3 and examined under optical microscope to ascertain the period as well as the stability of the domain structure period. Then the crystals with well-spaced domain structures were cut mechanically along the direction parallel to the laminar domains. The two light-transmitting surfaces, were mechanically ground to made parallel to laminar domains and then fine polished. The light-transmitting surfaces of sample is about 3x3 mm^2 and without antireflection coating.

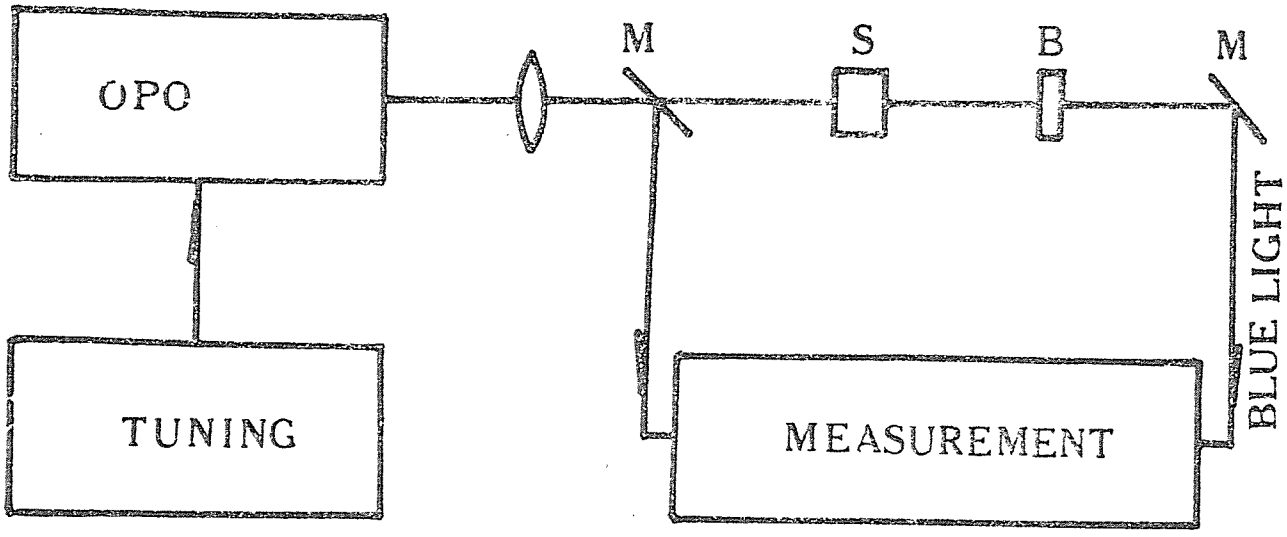

Fig. 3. The experimental setup for blue light generation.

The experimental setup is shown in figure 3. The fundamental pulse is obtained by employing a picosecond automatic tunable parametric oscillator laser with pulse rate of 1 pulse/s, in which pulse width is 30 ps, line width is less than 1 nm. The optical pulse from the laser is focused by a focusing lens into the crystal at where the

spot diameter is about 1 mm. Behind the sample, an infrared-cut filter is used to block the infrared light for blue pulse energy measurement. The SHG efficiency is the ratio of output energy to input energy.

2.2. Measurements of blue light as fundamental wavelength scanning

Figure 4 shows the phase-matching curve obtained by plotting the SHG efficiency while scanning the fundamental wavelength. The nonlinear optical coefficient d_{33} was addressed by polarizing the x-propagation fundamental wave linearly along the crystal z-axis. Figure 4a shows the curve of sample A in which QPM occured at 870 nm for d_{33}. Figure 4b is that of sample B in which QPM occured at 860 nm. Some parameters about samples and measured results are shown in table 3.

Table 3. Some parameters and measured results of sample A and sample B

	sample A	sample B
thickness	0.52 mm	0.78 mm
number of laminar domains	290	460
observed period	3.5 μm	3.4 μm
calculated period	3.52 μm	3.38 μm
wavelength for QPM	870 nm	860 nm
maximal SHG efficiency	3.5%	4.2%

From the table, the observed period L of sample A and B are 3.4 μm and 3.5 μm respectively. While the calculated

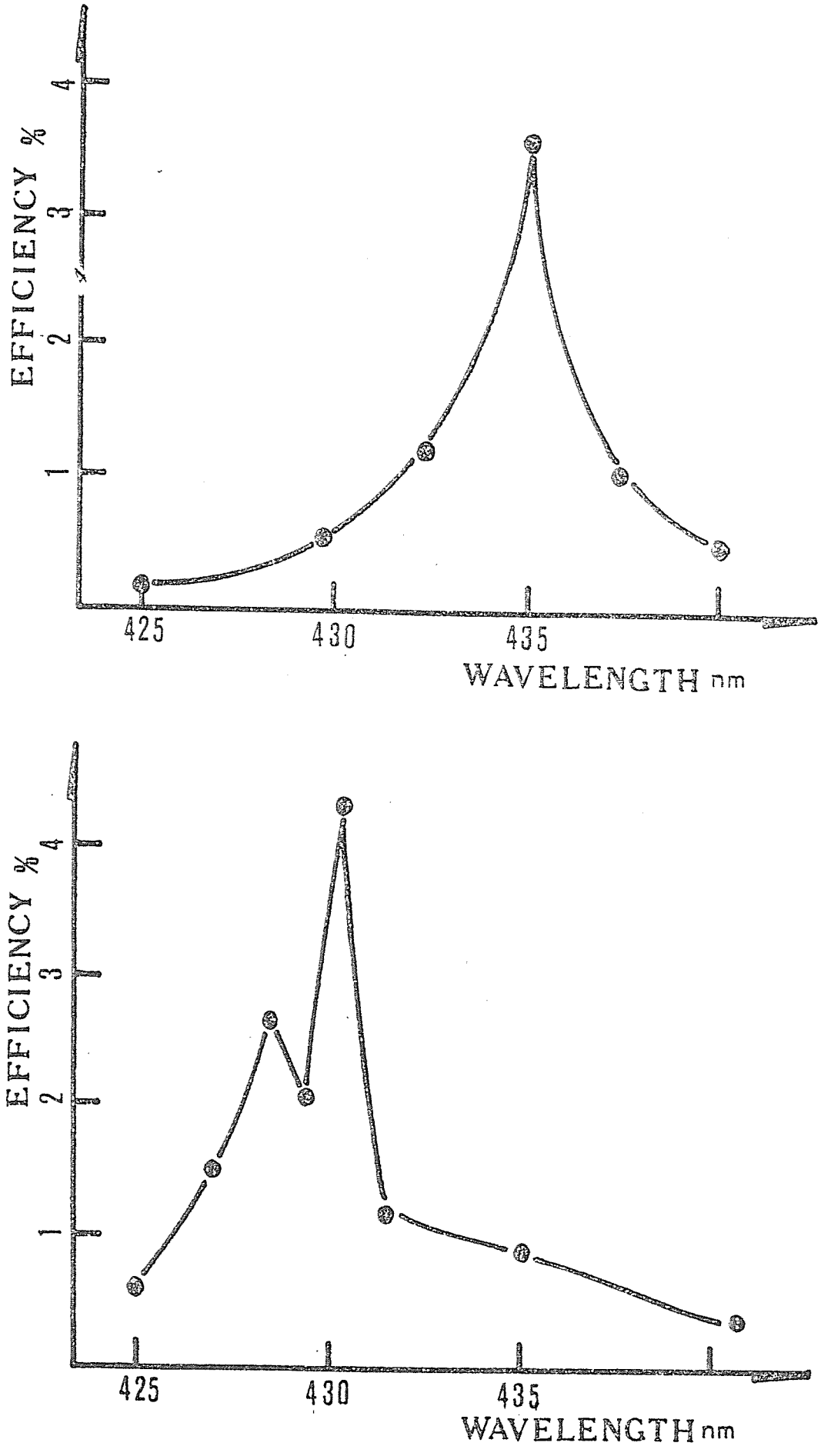

Fig. 4. The phase-matching curve for both : a), sample A. b), sample B.

coherence lengths l_c for fundamental wavelengths of 870 nm and 860 nm are 1.692 μm and 1.762 μm. The calculated period is the double of l_c. So it is easy to see that the calculated period is in good correspondence with the observed period.

The maximal conversion efficiencies of the two samples A and B are 3.5% and 4.2% respectively. These efficiencies were obtained by averaging ten laser pulses in which we dicarded those which have great discrepancy from the average input energy. The highest pulse conversion efficiency recorded was larger than 6.5%. In our measurements, the average input energy is 5 μj per pulse, mean power is about 0.17 mw. Using a 40 mm focusing lens, we estimated the power density was about 20 mw/cm^2. At this efficiency, we obtained 0.2 μj of blue light generation by the crystals. There are two maximal points (two peaks) in efficiency curve in figure 6b. It is due to inhomogeneity of the ferroelectric domain periodicity in $LiNbO_3$ crystals. For a exactly periodic domain structures, the maximum peak must be very sharp and SHG should be very highly efficient, according to the rule of square relation between SHG efficiency and domain laminar numbers. The dependence of the line shape of the efficiency curve and domain structures periodicity is a topic of current research in our laboratory. This corresponding relation is an important factor in evaluating whether a crystal is of good quality.

At the condition of QPM, $LiNbO_3$ crystal with periodic

ferroelectric doamin structures can be engineered to nonlinear interaction at any desired temperature, using any nonlinear optical coefficient, and involving any wavelength within the transparacy range of the crystal. Another important factor is that such a crystal has an improvement on photorefractive effect.[12] These merits of the crystal makes itself applicable to a much more wider variety of interactions. The work about compact, all solid-state blue laser is lust undergoing in our group.

2.3. Potential applications of QPM in waveguide

For bulk LN meterials, the QPM technique gives the possibility of achieving highly efficient frequency conversion, and thus , as we discribed in last section, opened a area of applications of the LN crystal for specially required frequency conversion process.

Potential applications of QPM will be in waveguide system. For blue light generation, for example, several approaches which included NPM, BPM and Cherenkov effect have been discribed. With the relatively low powers available from diode lasers, these approaches have generally required either a resonant/ or a waveguide structure to achieve the high conversion efficiencies needed for practical applications. Resonant systems require elaborate temperature and electric feedback techniques for maintaining stable operation[15]. For a waveguide systems, a guide length exceeding a milimeter is a prerequisite to efficient

conversion. However, such a length constitutes a formidable phase matching problem, limits the wavelength range, and puts extreme demands on waveguide fabrication[16]. For example, with device length of 1 mm, the refractive index mismatch between the fundamental and harmonic modes, Δn, must be kept constant within 0.001. For typical optical waveguide system. This requires waveguide depth fabrication tolerance to be less than 1nm over the sample length. This tolerance problem has been partially overcome by phase matching to the radiation mode (Cherenkov radiation scheme) but at the expense of complicated shaped output beams, tighter coupling requirements, and low conversion efficiencies[17].

With the using of QPM technique in periodic domain structure waveguide, formidable phase matching problem is not existed. Its high nonlinearity can reduce the effective waveguide length. It makes the fabrication tolerances much wider than that in waveguide systems described previously. It makes the QPM technique very useful not only in periodic domain structure LN waveguide, but also in other crystals such as in KTP.[18] The work about this aspect is in preparation in our group.

3. Concluding remarks

In this chapter, we discussed the blue light generation. Using the $LiNbO_3$ crystal with periodic domain structures, the measurements about SHG efficiency have been

systematically made. The highest efficiency of 4.2% was measured for picosecond blue light generation. This is the highest record of the results obtained in periodic-poled $LiNbO_3$ so far.

References:

1. J.T.Lin. Lasers & Optronics July.1989.PP61

2. J.T.Lin. SPIE Vol 1104 (1989)23

3. Laser focus world Apr. 1990 PP27

4. Laser & optronics July 1990. pp16

5. L.Goldberg and M.K.Chun, Appl. phys, lett. 55(1989)218

6. J.-C. Baumert and P.Gunter Appl.Phys.Lett. 50(1987)554

7. W.P.Risk, J.-C. Baumert Appl.phys.lett. 52(1988)85

8. L. Goldberg, M.K.Chun, L.N.Duling, T.F.Carruthers Appl. Phys. Lett. 56(1990)2071

9. T.Tohmon, K.Yamamoto, T.Taniuchi SPIE Vol.898 (1988)70

10. T.Taniuchi, and K.Yamamoto ECOC'89 (1986)171

11. G.Tohomon, K.Yamamoto, T. Taniuchi SPIE v.898(1988) 70

12. A. Magel, M.M. Fejer, R.L.Byer Appl. Phys. Lett. 56(1990)108

13. E.L. Lim et. al. CLEO'89 paper ThQ3(1989)

14. D. Feng, N. B. Min, J.F.Hong,Y.S.Yang Appl.phys.lett. 37(1980)607

15. W. J. Kozlovsky, W.Lenth, E.E. Latta Appl.phys.lett. 56(1990)2991

16. F. Laurell and G.Arvidssen J. Opt. Soc. Am. B5(1988)292

17. T.Taniuchi,and K.Yamamoto 12th ECOC,Vol.1 (1986)22

18. C. T. Van der poel, J.D.Bierlein, J.B.Brown Appl. Phys. Lett. 57(20) (1990) 2074

Chapter 5 Optical Parametric Oscillation

1. Introduction

1.1 Brief historical review

The optical parametric oscillator (OPO) is a device which produces intense optical radiation possessing a high degree of spatial and temporal coherence. The radiation OPO emitted is as spectrally pure as that emitted by a laser and may be tuned over a wide range. In addition the optical parametric oscillator can be in continuous as well as in pulsed operation.

Interest in optical parametric interactions began with the observation of optical second-harmonic generation by Franken et al[1], which shown that optical frequency nonlinearity existed. This in turn was made possible by the successful operation of the first laser by Maiman in 1960[2]. In 1962 several proposals for tunable optical parametric oscillators were made by Akhmanov, kingston et.al.[3-5]. In the same year Giordmain[6] and Maker[7] et. al. introduced the concept of phase matching which permitted much strong nonlinear interactions. In 1964 the first of a number of new nonlinear optical materials, $LiNbO_3$, was introduced by Boyd et.al.[8]. The first pulsed optical parametric oscillator was successfully operated by Giordmain and Miller in 1965[9]. Following this first oscillator a number of other pulsed oscillator were constructed. In 1966 it was shown that optical parametric oscillation could in principle be achieved on a continuous basis in Boyd and Ashkin's

thoery[10] and in 1968 successful continuous operation of optical parametric oscillators were obtained by Smith and Byer et.al in 1968.[11-12]. The progress in this field before 1975 has been reviewed by Byer[13].

Table 1 list some typical experiments on parametric oscillator since 1970. In which except the materials such as KDP, $LiNbO_3$, BNN and ADP, the oscillation were also constructed in some new nonlinear materials, such as urea, $KNbO_3$ and BBO.

Table 1 . Pulsed OPO experiments.

Pump	Material	output power and linewidth	tuning range	efficiency
0.532um	$LiNbO_3$	0.1-10kW --200ns	0.55-3.65 μm	45%
0.532um	KDP	30ps	0.9-1.3μm	50%
0.532um	KDP	100kW 20ns	0.957-1.17μm	3%
0.355um	ADP	100kW 20ns	0.42-0.73μm	25%
0.532um	α-HIO_3	10MW 20ns	0.68-2.4μm	10%
0.6943um	$LiIO_3$	100kw 15ns	1.1-1.9μm	10%
0.532um	$KNbO_3$	10ns	0.88-1.35μm	25%
0.355um	urea	10ns	0.49-1.20μm	25%
0.532um	BBO	12ns	0.94-1.22μm	10%

Table 2 also list some experiments in $LiNbO_3$ OPO which

have been achieved so far.

Table 2 . $LiNbO_3$ OPO operating parameters

Tuning range (um)	peak power (W)	average power (mW)	pulse length (ns)	pumping (λm)
3.5-2.5	80-150	5-10	70	0.532
0.975-2.5	250-350	30	80	0.659
0.725-0.975	250	20	240	0.562
0.623-0.760	250	50	150	0.532
0.546-0.593	300	3-5	200	0.473

In addition to the results aforementioned, a lot of work have been done in achieving higher power and higher efficiency, exploring new oscillator configurations and obtaining greater tuning ranges, narrow spectral linewidth and smooth tuning.

1.2 Materials

Nonlinear materials used for optical parametric oscillator have, in general, the same properties and requirements as those materials used for optical second-harmonic generation. These requirements and desirable properties are:

1). lack a center of symmetry,

2). possess a large value of d^2/n^3,

3). be phase-matchable,

4). be transparent for all wavelengthes of interest,

5). be homogeneous and of good optical quality,

6). be high resistant to optical damage.

Some of the materials in which parametric amplification or oscillation have been observed and materials which appear promising for such applications are listed in table 3, along with their characteristic parameters, such as the fiqure-of-merit, and transparent range.

Table 3. Properties of some materials used for OPO

Material	d^2/n^3(esu)	transparent range(μm)
BBO	$6*10^{-18}$	0.19-3
KDP	$0.4*10^{-18}$	0.2-1.3
ADP	$0.55*10^{-18}$	0.2-1.15
$LiIO_3$	$28*10^{-18}$	0.4-4
$LiNbO_3$	$14*10^{-18}(d_{22})$	0.35-4.5
	$225*10^{-18}(d_{eff},QPM)$	
BNN	$95*10^{-18}$	0.4-4
Ag_3AsS_3	$50*10^{-18}$	0.64-10
CdSe	$300*10^{-18}$	1-15
-HgS	$500*10^{-18}$	0.6-13
Se	-10^{-14}	0.8-25
Te	$-4*10^{-13}$	5-25

For oscillators which cover the red and infrared regions, LN, BNN, LI are the most promising materials. BNN and LI have very high optical damage threshold at above room temperature. LI is a water-soluble crystal and is not durable as the niobate's. It can, however, be grown with high optical quality as KDP and ADP. Surface damage has been seen in LI, BNN, and LN as well as in other nonlinear materials.